Heliyon 9 (2023) e20105

Contents lists available at ScienceDirect

Heliyon

journal homepage: www.cell.com/heliyon

Carboxyamidotriazole alleviates pannus formation and cartilage erosion in rats with adjuvant arthritis

Yongting Zhou, Xiyue Yang, Jingwen Liu, Mei Yang, Caiying Ye, Lei Zhu *

Department of Pharmacology, Institute of Basic Medical Sciences, Chinese Academy of Medical Sciences and School of Basic Medicine, Peking Union Medical College, Beijing 100005, PR China

ARTICLE INFO

Keywords:
Carboxyamidotriazole
Adjuvant arthritis
Angiogenesis
Matrix metalloproteinase
Mitogen-activated protein kinases
Fibroblast-like synoviocyte

ABSTRACT

Carboxyamidotriazole (CAI) was initially considered a non-cytotoxic anticancer agent. However, recently, pronounced anti-inflammatory properties of CAI have been reported. Rheumatoid arthritis (RA) is an autoimmune inflammatory disease characterized by aberrant activation of signaling pathways. Therefore, this study explored the therapeutic effects and potential mechanism of action of CAI on RA in the adjuvant arthritis (AA) model. The results showed that CAI reduced the severity of arthritis in AA rats as demonstrated by inhibited hind paw swelling, reduced body weight, and decreased infiltration of joint pathological inflammatory cells. Importantly, pathological scoring of new blood vessels and immunohistochemical assays revealed that CAI inhibited pannus formation. CAI decreased the expression of pro-angiogenic growth factors, such as vascular epidermal growth factor, basic fibroblast growth factor, and metalloproteinases (MMPs), namely, MMP-1 and MMP-3 in the synovium of AA rats. Furthermore, CAI significantly reduced the increased levels of phosphorylated p38, c-Jun N-terminal kinase (JNK) 1/2, and extracellular signal-regulated kinase (ERK)1/2 proteins in AA rats. In addition, the proliferation of fibroblast-like synoviocytes (FLS) was downregulated by CAI both *in vivo* and *in vitro*. In conclusion, this investigation illustrates the therapeutic effect of CAI on synovitis and erosion of articular cartilage in RA. Furthermore, the mechanism might involve inhibition of aberrantly activated mitogen-activated protein kinase signaling, as well as a decrease in pro-angiogenic factors, MMP expression, and FLS proliferation.

1. Introduction

Rheumatoid arthritis (RA) is a systemic autoimmune disease characterized by the chronic progressive swelling and destruction of multiple joints. RA frequently results in disability, systemic complications, and early death, and has a high socioeconomic burden. The precise progression of RA is unknown; however, immune disorders, pannus formation, and cartilage lesions are principally involved [1].

Protection against joint deformation and destruction can be an important means of improving the quality of life of patients with RA [2]. Immune cells and fibroblast-like synoviocytes (FLS) play synergistic and mutually reinforcing roles in the pathogenesis underlying bone damage in RA [3].

* Corresponding author. Department of Pharmacology, Institute of Basic Medical Sciences, Chinese Academy of Medical Sciences and School of Basic Medicine, Peking Union Medical College, Beijing 100005, China.
E-mail address: zhulei@ibms.pumc.edu.cn (L. Zhu).

https://doi.org/10.1016/j.heliyon.2023.e20105
Received 30 November 2022; Received in revised form 22 August 2023; Accepted 12 September 2023
Available online 14 September 2023

The mitogen-activated protein kinase (MAPK) signaling pathway is actively involved in regulating synovial inflammation and joint destruction and plays an important role in the pathogenesis of RA. Activated MAPK pathway proteins, including p38, c-Jun N-terminal kinase (JNK), and extracellular signal-regulated kinase (ERK), mediate the expression of several downstream genes that play important roles in the regulation of synovial inflammation, hyperplasia, matrix degeneration, and bone erosion [4]. Furthermore, inhibitors targeting the MAPK pathway significantly improve disease progression in adjuvant arthritis (AA) rats [5].

In healthy joints, FLS controls the composition of the extracellular matrix (ECM) and synovial fluid; however, it exhibits a unique aggressive behavior in RA joints. Immune cells release inflammatory cytokines and growth factors, such as vascular epidermal growth factor (VEGF) and basic fibroblast growth factor (bFGF), which act as important regulatory mediators that stimulate differentiation of FLS into proinflammatory and tissue-damaging subsets [1,6]. Excessive accumulation of inflammatory cytokines produced by FLS is a major contributor to synovial inflammation, joint pain, and swelling in patients with RA. In addition, excess proteases, such as matrix metalloproteinases (MMPs), released into the synovial fluid can attack normal joints and degrade the collagenous cartilage matrix, causing damage [7]. FLS also have proliferative properties similar to tumor cells and can break through the physiological barrier to invade the cartilage, leading to joint erosion. More importantly, new blood vessels, proliferating synovial cells, and inflammatory cells form the pannus, releasing harmful enzymes, acids, and proteins that damage the bone and cartilage, which may lead to permanent joint deformity [8].

Although the clinical agents used in patients with RA, such as nonsteroidal anti-inflammatory drugs (NSAIDs) and disease-modifying antirheumatic drugs (DMARDs), can alleviate symptoms, their side effects, such as gastric ulcers, hypertension, hepatotoxicity, and renal abnormalities, restrict their use in the treatment of RA [9]. Moreover, the existing therapies for RA are not capable of completely preventing structural damage or restoring joint erosion. Therefore, novel, effective, and safe treatment strategies are urgently needed. Carboxyamidotriazole (CAI) was originally developed as a non-cytotoxic anticancer drug, but a variety of studies have shown the anti-inflammatory effect of CAI. A previous study reported that CAI reduced the production of cytokines at the site of inflammatory tissues and serums in AA rats *in vivo*, mechanically impeding the phosphorylated inhibitor of nuclear factor-κBα (IκBα) and NLRP1 inflammasome activation [10]. In addition, CAI inhibited cytokine release by blocking MAPK pathway activation, which was assayed using RAW264.7 macrophages *in vitro* [11]. However, it remains unclear whether CAI improves joint and cartilage destruction and the related mechanisms in RA.

Here, we conducted a pharmaceutical study in rats with adjuvant arthritis (AA) and demonstrated the protective role of CAI against joint inflammation and cartilage damage. In an action mechanism study, we demonstrated that CAI suppressed MAPK activation, angiogenic factors, MMP expression, and FLS proliferation, all of which play vital roles in the pathogenesis of RA.

2. Materials and methods

2.1. Animals

Female Lewis rats (180–210 g, Beijing Vital River Laboratory Animal Co., Ltd.) were housed under controlled standard conditions (22 ± 2 °C temperature, 12 h light/dark cycle and 40–60% humidity). Food and water were provided ad libitum. All animal experiments were approved by the Institutional Animal Care and Use Committee of Chinese Academy of Medical Science (ACUC-A02-2021-027).

2.2. Drugs and reagents

CAI was synthesized by the Institute of Materia Medica, Chinese Academy of Medical Sciences (>99% by high-performance liquid chromatographic purity test). It was dissolved in dimethyl sulfoxide (DMSO) as a 40 mM stock for *in vitro* experiments and in polyethylene glycol 400 (PEG 400) at required concentration for *in vivo* experiments. Dexamethasone sodium phosphate injection was provided by Tianjin Jinyao Amino Acid Company (Tianjin, China). PEG 400 was purchased from Beijing Chemical Reagents Company (Beijing, China); Mycobacterium tuberculosis, from National Vaccine & Serum Institute (Beijing, China); Protease Inhibitor Mix was from Roche (Basel, Switzerland); Peroxidase Substrate DAB kit was purchased from abcam (Cambridge, MA, USA); enhanced chemiluminescence reagent was provided by merck Millipore(Billerica, MA, USA); Cell Counting Kit-8 (CCK-8) was from dojindo (Kumamoto, Japan); primary antibody against CD31, from Abcam (Cambridge, MA, USA); primary antibodies against phospho-JNK1/2, JNK1/2, phospho-p38, p38, phospho-ERK and ERK, from Cell Signaling Technology (Beverly, MA, USA); primary antibodies against MMP-1, MMP-3, VEGF, bFGF, β-actin and peroxidase-conjugated secondary antibodies, from Santa Cruz Biotechnology (Santa Cruz, CA, USA). Dulbecco's modified Eagle's medium (DMEM) from Gibco Co. (CA, USA) was supplemented with 10 mM HEPES, 2 mM L-glutamine, 100 units/ml penicillin and 100 μg/ml streptomycin. Other chemicals used in these experiments were analytical grade from commercial sources.

2.3. Induction and evaluation of AA

Complete Freund's adjuvant (CFA) was prepared by suspending heat-killed Mycobacterium tuberculosis in mineral oil at 10 mg/ml. AA was induced by a single subcutaneous injection of 0.1 ml CFA at the base of the tail of rats. Non-arthritic group rats were injected with 0.1 ml of mineral oil alone. The onset and severity of arthritis were inspected daily by two observers who were blinded to the treatment. The hind paw volumes were determined with a plethysmometer chamber before immunization (baseline, day 0) and at 2-day intervals from day 12–26 after immunization. The paw swelling (Δml) was expressed by subtracting the paw volume at day

0 from that after immunization. And the mean Δml of both hind paws was calculated for each rat. First signs of inflammation started to develop on about day 10–12 after immunization. During the experimental period, the body weight of rats was measured using a digital weighing balance before immunization (day 0) and daily from day 12 to day 26 after CFA injection.

2.4. Drug treatment

Before the experiment, Lewis rats were randomly divided into seven groups with 14 animals in one group. The rats with AA were administered with CAI (10, 20 and 40 mg/kg, i.g.), dexamethasone (0.2 mg/kg, i.p.), or vehicle (PEG 400, i.g. and normal sodium (N. S.), i.p.) once daily from day 12–26 post-CFA injection.

2.5. Swelling dimension observation of knee joint

The hind paws of rats were measured by YLS-7B plethysmometer (Shandong Province Academy of Medical Science, Jinan, China). The hind paw volume was measured by dipping the foot into the water bath up to the line drawing in lateral malleolus. The increase in percentage of paw volume was calculated based on the volume difference between the normal and abnormal paws [12].

2.6. Histological examination

Rats were sacrificed by cervical dislocation after ether anesthesia on day 26 after immunization. The knee joints were fixed in 10% phosphate-buffered formalin, decalcified in 10% EDTA for 14 days at 4 °C, then embedded in paraffin. Serial paraffin sections (4 μm) were stained with hematoxylin and eosin (H&E). All sections were scored histologically by two independent observers, as described previously [13]: 0 = normal joint; 1 = normal synovium with occasional mononuclear cells; 2 = definite arthritis, a few layers of flat to rounded synovial lining cells and scattered mononuclear cells; 3 = clear hyperplasia of the synovium with three or more layers of loosely arranged lining cells and dense infiltration with mononuclear cells; 4 = severe synovitis with pannus and erosions of articular cartilage and subchondral bone.

For the quantitative analysis of new blood vessels, the identical location of knee joint in different individuals was selected for observation. The number of new blood vessels localized in synovial lining was counted by two investigators blinded to the experimental groups under microscope (200X). Two sections of every joint (n = 4 rats per group) were taken at different depths, and 5 microscopic fields were counted for each section.

2.7. Immunohistochemistry

The paraffin-embedded synovium sections were deparaffinized for immunohistochemical staining of CD31 and VEGF. Endogenous peroxidase activity was blocked using 3% H_2O_2 for 10 min, followed by incubation with non-specific staining blocking reagent for 10 min. The sections were incubated with the optimal dilutions of anti-CD31 (1:50) and anti- VEGF (1:50) antibodies overnight at 4 °C followed by 1 h with horseradish peroxidase (HRP)-labeled secondary antibodies. Immune complexes were visualized with Peroxidase Substrate DAB kit. Hematoxylin was used for nuclear counterstaining. The quantitative assay for the positive staining cells was the same as that described in new blood vessel count.

2.8. Western blot analysis

Synovial tissues were homogenized in ice-cold lysis buffer (50 mM Tris-HCl, 150 mM NaCl, 0.1% sodiumdodecylsulfate (SDS), 1% Nonidet P-40, 0.5% sodium deoxycholate, 1 mM EDTA, 1% Protease Inhibitor Mix, PH 7.4). The lysates were centrifuged at 14,000×*g* for 15 min at 4 °C. The supernatants were collected and the protein concentrations were determined using the Bradford method. Equivalent amounts of protein (40 μg) were electrophoresed on 12.5% SDS-polyacrylamide gel electrophoresis and transferred to polyvinylidene fluoride membranes using standard techniques. Membranes were blocked for 1 h at room temperature with 5% nonfat dry milk in Tris-buffered saline (50 mM Tris-HCl, 150 mM NaCl, 0.05% Tween-20, pH 7.5) and incubated with individual primary antibodies at 4 °C overnight. Then they were incubated with horseradish peroxidase-coupled secondary antibodies. The immunoreactive proteins were detected with enhanced chemiluminescence reagent using Fujifilm Las-3000 Luminescent Image Analyzer and quantified using Kodak 1D software.

2.9. Isolation and culture of FLS

Rats were anaesthetized and sacrificed on day 26 after immunization. Fresh synovial membrane tissues of knee joints were obtained and washed thoroughly with phosphate-buffered saline (PBS). Tissues were minced into 1–2 mm^3, and digested in DMEM containing 1 mg/ml collagenase type IV and 10% fetal bovine serum (FBS) at 37 °C in a humidified atmosphere of 5% CO2 for 2 h. The digested tissues were filtered using a 200 mesh (75 μm) filter and the resulting cell suspension was centrifuged at 1500 × rpm (352×*g*) for 10 min using Kecheng low-speed centrifuge. The cell pellets were washed twice and then incubated in DMEM containing 10% FBS at 37 °C, 5% CO2. After 24 h, the adherent cells (FLS) were cultured in the fresh medium, and non-adherent cells were discarded. When the cells had grown to 80% confluence they were detached with 0.25% trypsin and split in 1:3 ratios. All experiments were performed using cells within passages 3–6.

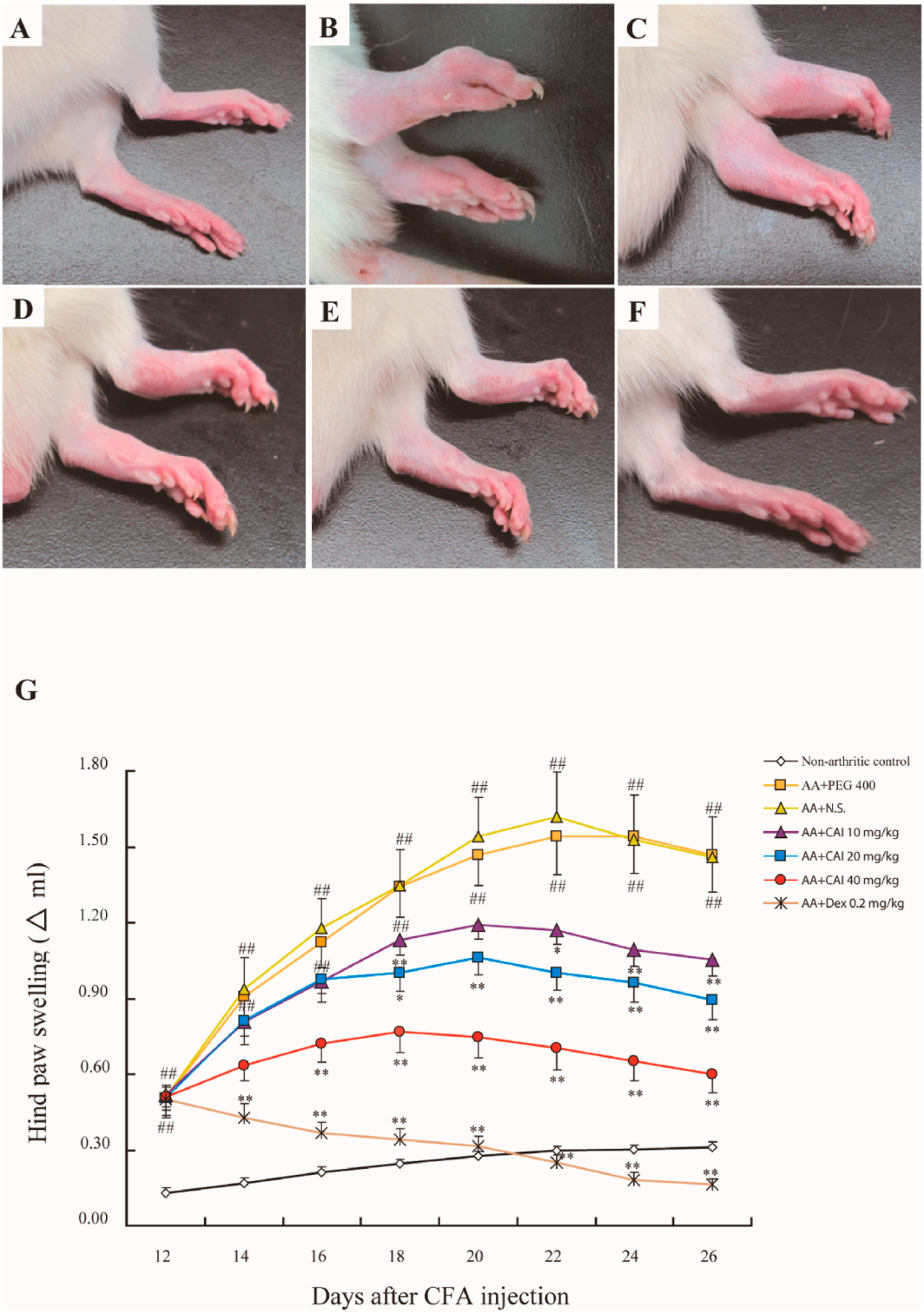

Fig. 1. Effects of CAI on paw swelling in AA rats. AA was induced by a single subcutaneous injection of 0.1 ml of CFA at the base of the tail on day 0. CAI (10, 20, 40 mg/kg/) and Dex (0.2 mg/kg) were given from day 12–26 after immunization. Hind-paw swelling (Δ ml) was assessed by determining increases in hind-paw volume, as described in Materials and methods. Ã F: representative photographs of the hind paws from each group taken on day 26 after immunization. A: the normal group, B: vehicle PEG 400 -treated AA group, C: vehicle N.S.-treated AA group, D: CAI 20 mg/kg-treated AA group, E: CAI 40 mg/kg-treated AA group, F: Dex-treated AA group. G: Δ ml of the hind paws are presented as the mean and SEM of 14 rats per group. $^{\#\#}P < 0.01$ vs. non-arthritic control group, $^{*}P < 0.05$, $^{**}P < 0.01$ vs. vehicle-treated AA group.

2.10. FLS proliferation assay

FLS proliferation was determined by CCK-8 method. Briefly, FLS isolated from the paw of arthritic rats were plated into 96-well plates in triplicate at 2×10^4 cells/well and incubated for 24 h at 37 °C, 5% CO2 until cells adherence. To investigate the effect of

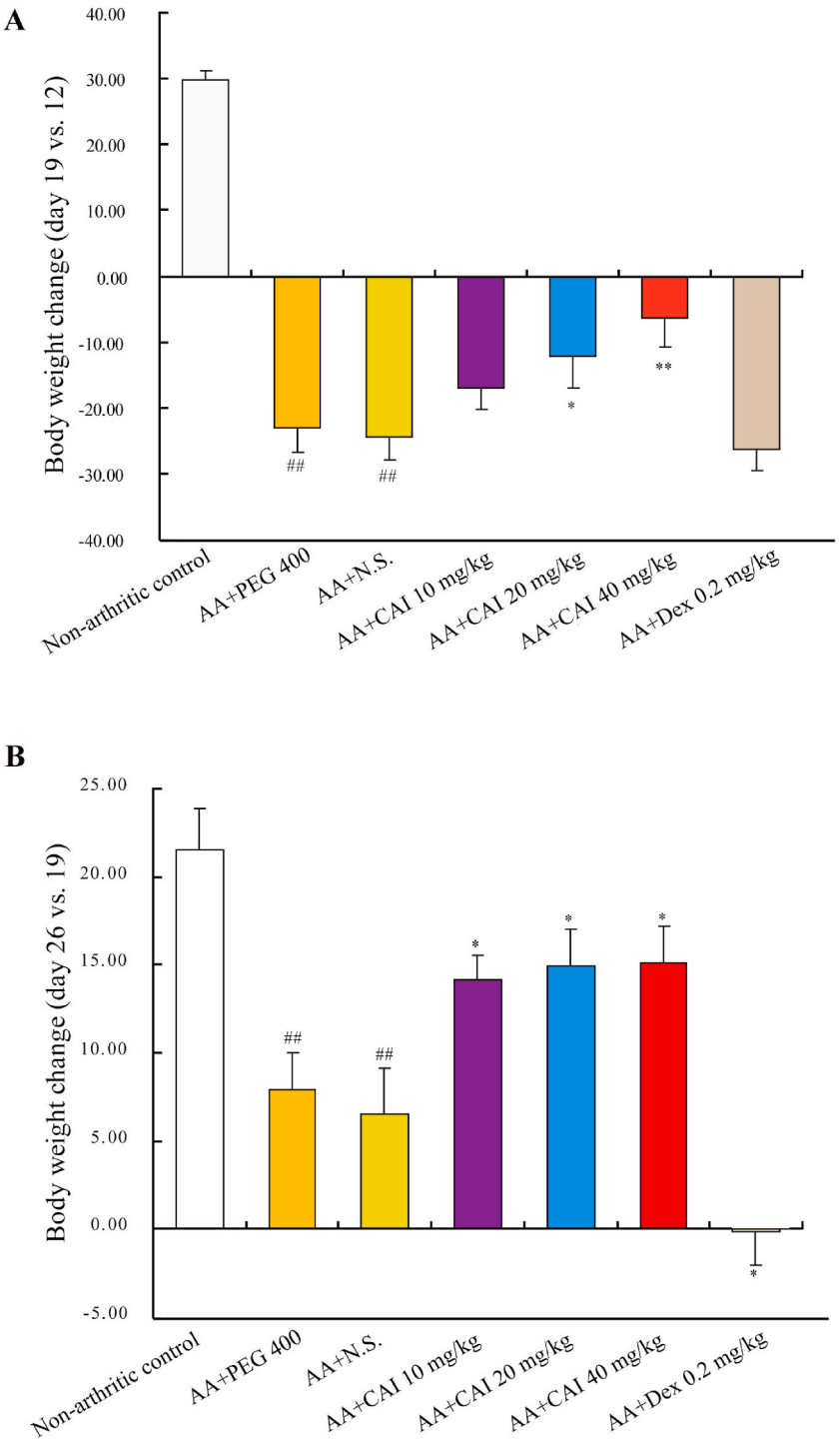

Fig. 2. Effect of CAI on adjuvant-induced weight loss in rats. A: changes in body weight during the first week of treatment (from day 12–19). B: changes in body weight during the second week of treatment (from day 19–26). Values are the mean and SEM of 14 rats per group. $^{\#\#}P < 0.01$ *vs.* non-arthritic control group, $^{*}P < 0.05$, $^{**}P < 0.01$ *vs.* vehicle-treated AA group.

CAI on AA FLS proliferation *in vivo*, the culture medium of FLS from different group rats was replaced by 200 μl fresh medium. To investigate the effect of CAI on AA FLS proliferation *in vitro*, the culture medium of AA FLS was replaced with 200 μl fresh medium containing desired concentration of CAI (5, 10, 20, 40 μM), or a vehicle control consisting of 0.1% DMSO. After incubation for 48 h, 20 μl CCK-8 solution was added into each well and further incubated for 3 h. The absorbance (A) at 450 nm was measured using a BioTek MQX200 microplate spectrophotometer.

2.11. Statistical analysis

Data are expressed as mean ± SEM. Statistical analysis was determined using GraphPad Prism software. Statistical evaluation involved one-way analysis of variance (ANOVA) followed by Bonferroni multiple comparison test. The value P less than 0.05 was regarded statistically significant (*, $^{\#\#}P < 0.05$ and **, $^{\#\#}P < 0.01$).

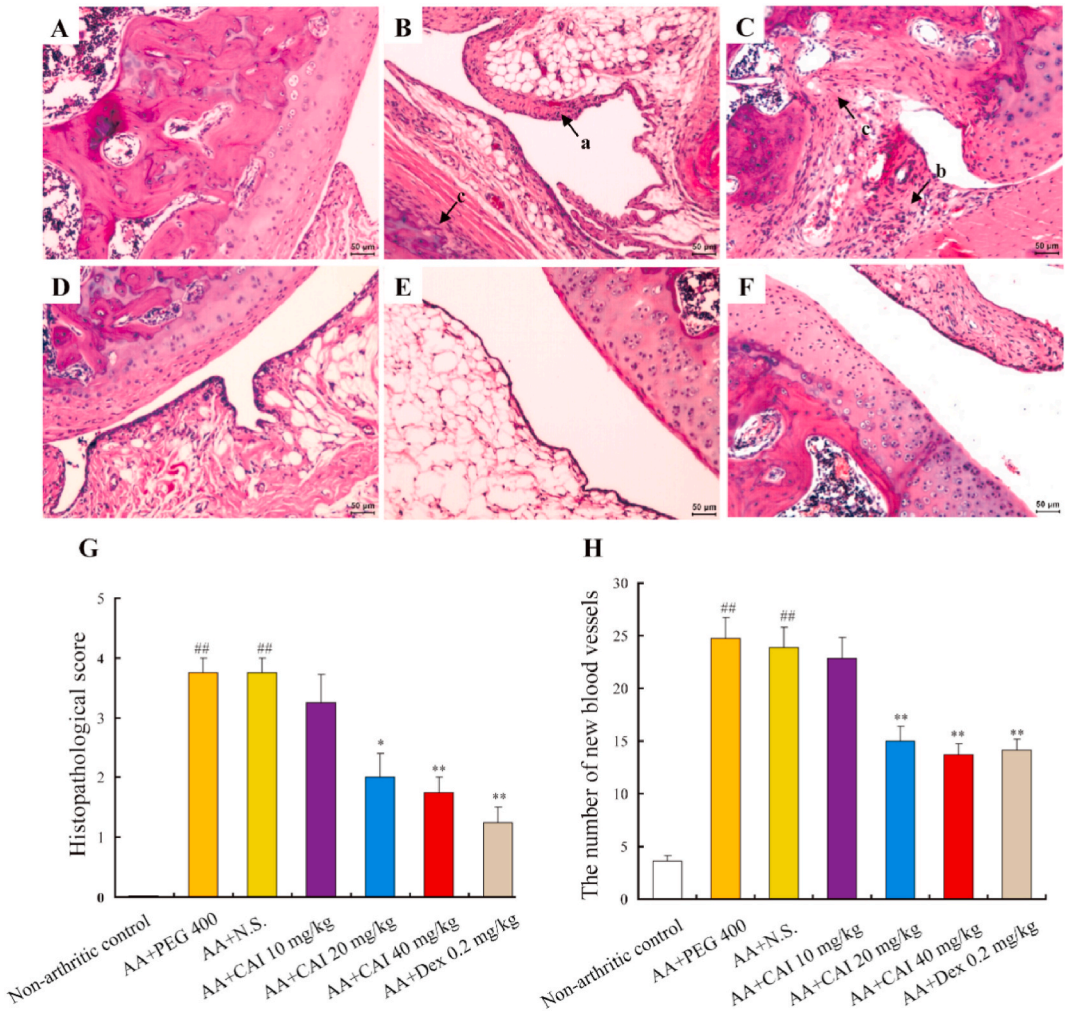

Fig. 3. Histopathological assessment of AA rats. Ã F: representative images of H&E-staining sections from the normal rats (A), vehicle PEG 400 -treated AA rats (B), vehicle N.S.-treated AA rats (C), CAI 20 mg/kg-treated AA rats (D), CAI 40 mg/kg-treated AA rats (E), and Dex-treated AA rats (F) (original magnification × 200, bars = 50 μm). Note the synovial hyperplasia (a), inflammatory cell infiltration (b) and pannus formation resulting in cartilage-bone erosions (c) in vehicle-treated AA rats. In contrast, the above histological changes were ameliorated in CAI (20, 40 mg/kg) and Dex group. G: histopathological score. H: new blood vessels were counted in H&E-staining sections, as described in Materials and methods. Values in G and H are the mean and SEM of n = 4 rats in each group. $^{\#\#}P < 0.01$ *vs.* non-arthritic control group, $^{*}P < 0.05$, $^{**}P < 0.01$ *vs.* vehicle-treated AA group.

3. Results

3.1. Effects of CAI on paw swelling in AA rats

Inflammatory arthritis was induced in all the immunized rats. The peak incidence occurred on day 12 after immunization (Fig. 1A and B). CAI (10, 20, and 40 mg/kg/day, i.g., × 14 days) was administered from that interval (day 12). It (10 mg/kg) reduced paw swelling on days 22, 24, and 26 (Fig. 1C and G). From days 18–26 and days 16–26, CAI doses of 20 mg/kg and 40 mg/kg significantly suppressed paw swelling, respectively, compared to the effects observed in vehicle PEG 400-treated AA rats (Fig. 1D, E and G). The positive control Dex (0.2 mg/kg), almost completely inhibited the development of paw swelling from day 14 after CFA injection (Fig. 1F and G).

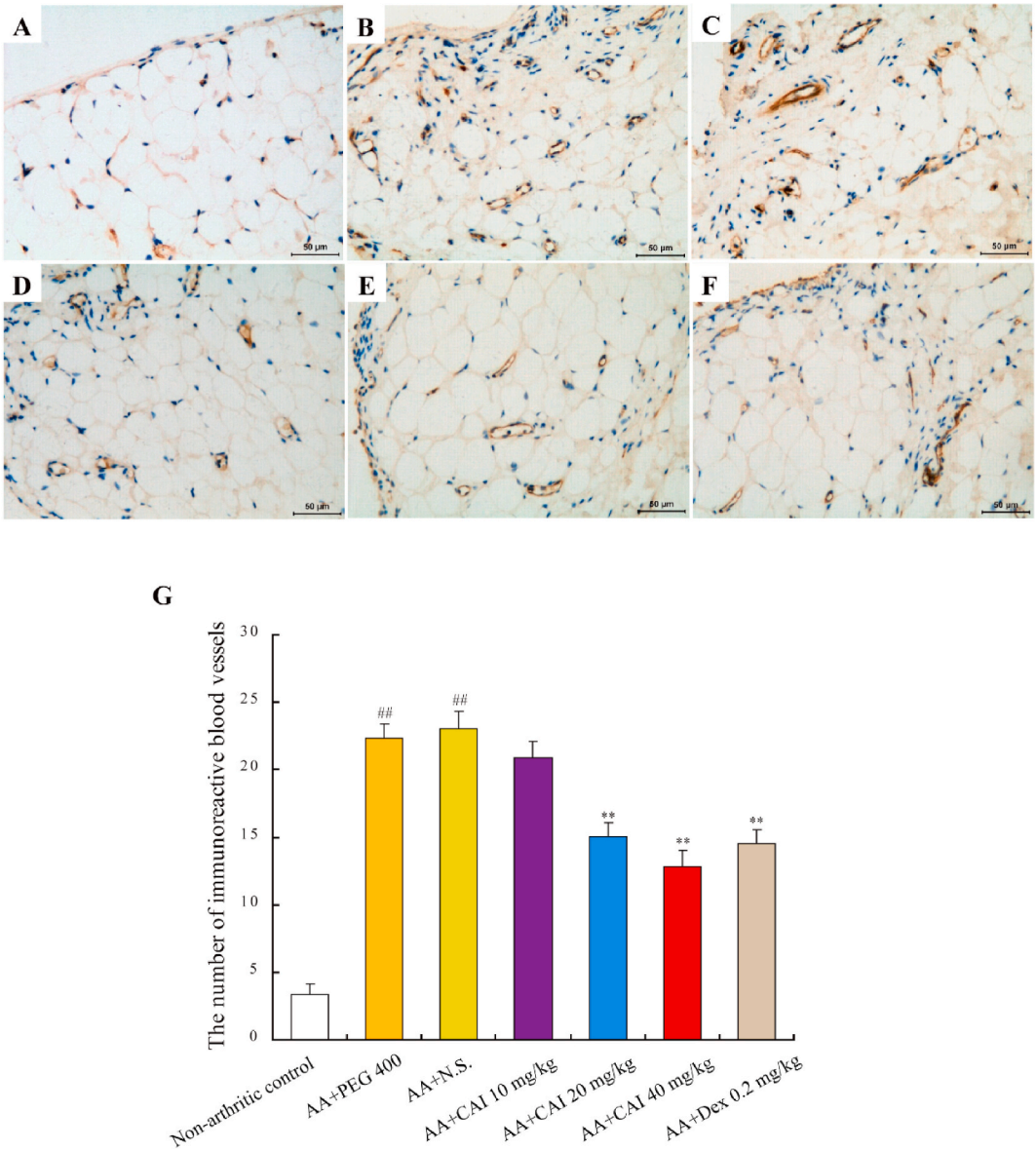

Fig. 4. CAI suppressed angiogenesis of synovial lining in AA rats. The synovium was immunohistochemical stained with anti-CD31 antibody to identify blood vessels. Ã F: representative immunostaining sections from the normal rats (A), vehicle PEG 400 -treated AA rats (B), vehicle N.S.-treated AA rats (C), CAI 20 mg/kg-treated AA rats (D), CAI 40 mg/kg-treated AA rats (E), and Dex-treated AA rats (F) (original magnification × 200, bars = 50 μm). G: quantitative data for the number of new blood vessels expressing CD31 in synovial tissue. Values are the mean and SEM of 4 rats per group. $^{\#\#}P < 0.01$ *vs.* non-arthritic control group, $^{**}P < 0.01$ *vs.* vehicle-treated AA group.

3.2. Effects of CAI on adjuvant-induced weight loss in rats

A significant decrease in body weight was observed between days 12 and 19 in AA rats compared to that in normal rats. The administration of CAI (20 and 40 mg/kg) from days 12–19 ameliorated the loss of body weight in AA rats (Fig. 2A). Continuation of CAI (10, 20, and 40 mg/kg) administration until day 26 resulted in a significant increase in the weight of AA rats compared to that on day 19. In the three groups of CAI-treated AA rats, a marked increase in weight was observed compared to that of the vehicle PEG 400-treated AA group on day 26 (Fig. 2B). However, Dex (0.2 mg/kg) had no effect on body weight loss of AA rats during the first week of treatment (from day 12–19) (Fig. 2A). Furthermore, the body weight of rats in the Dex group was lower than that of the vehicle N.S.-treated AA rats during the second week of treatment (from day 19–26) (Fig. 2B).

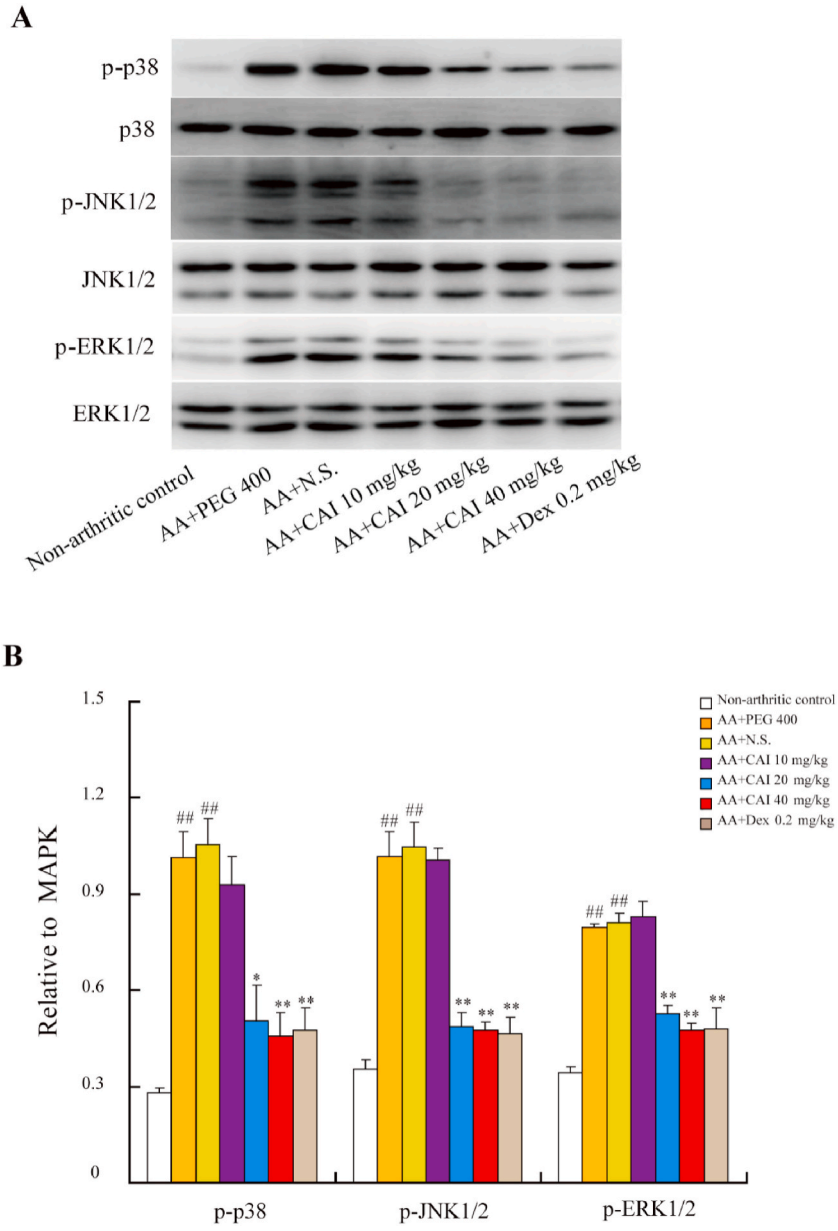

Fig. 5. Effect of CAI on MAPK pathway in AA rats. A. Western blot analysis of the p and total levels of p38, JNK, and ERK in rats treated with different CAI concentration (original image seeing in supplementary Fig. 5A). B. Bar graphs show quantitative evaluation of p and total levels of p38, JNK, and ERK bands by densitometry from triplicate independent experiments. $^{\#\#}P < 0.01$ *vs.* non-arthritic control group, $^{*}P < 0.05$, $^{**}P < 0.01$ *vs.* vehicle-treated AA group.

3.3. Effects of CAI on the histopathology of AA rats

Macroscopic observations were confirmed by histological examination. Compared with the normal joint architecture (Fig. 3A), the joints of vehicle-treated AA rats showed signs of severe arthritis, such as synovial hyperplasia, inflammatory cell infiltration of the synovial lining layer, extensive angiogenesis, pannus formation, cartilage degradation, and subchondral bone erosion (Fig. 3B and C). After 14 days of treatment, the degree of histopathological damage was significantly reduced in AA rats that were administered CAI (20 and 40 mg/kg) or Dex (0.2 mg/kg) (Fig. 3D–F), and the histological score was much lower than that of the vehicle-treated AA group (Fig. 3G).

3.4. Effects of CAI on angiogenesis of synovial lining in AA rats

Angiogenesis, the formation of new blood vessels from preexisting vessels, plays a prominent role in pannus formation in RA. To elucidate how CAI exerted its anti-arthritic effects, the formation of new blood vessels was observed, and their number was counted in H&E-stained sections of the synovial tissues. A few new blood vessels were observed in the synovial lining of normal rats. The number of new blood vessels in the hyperplastic synovium of AA rats significantly increased. However, the number of new blood vessels was lower in the thin synovial tissue of rats treated with CAI (20 and 40 mg/kg) or Dex (0.2 mg/kg) than that in the AA control (Fig. 3H).

To confirm the histopathological count of new blood vessels in the H&E-stained sections, the expression of CD31, a marker used to visualize angiogenesis, was determined by immunostaining. As shown in Fig. 4A, B and G, the immunoreactive blood vessels markedly increased in the synovial tissues of vehicle PEG 400- and N.S.-treated AA rats compared to those in the normal rats, which was consistent with the results of H&E staining. Interestingly, new blood vessels were significantly reduced in the synovium of AA rats treated with CAI (20 and 40 mg/kg) (Fig. 4D and E).

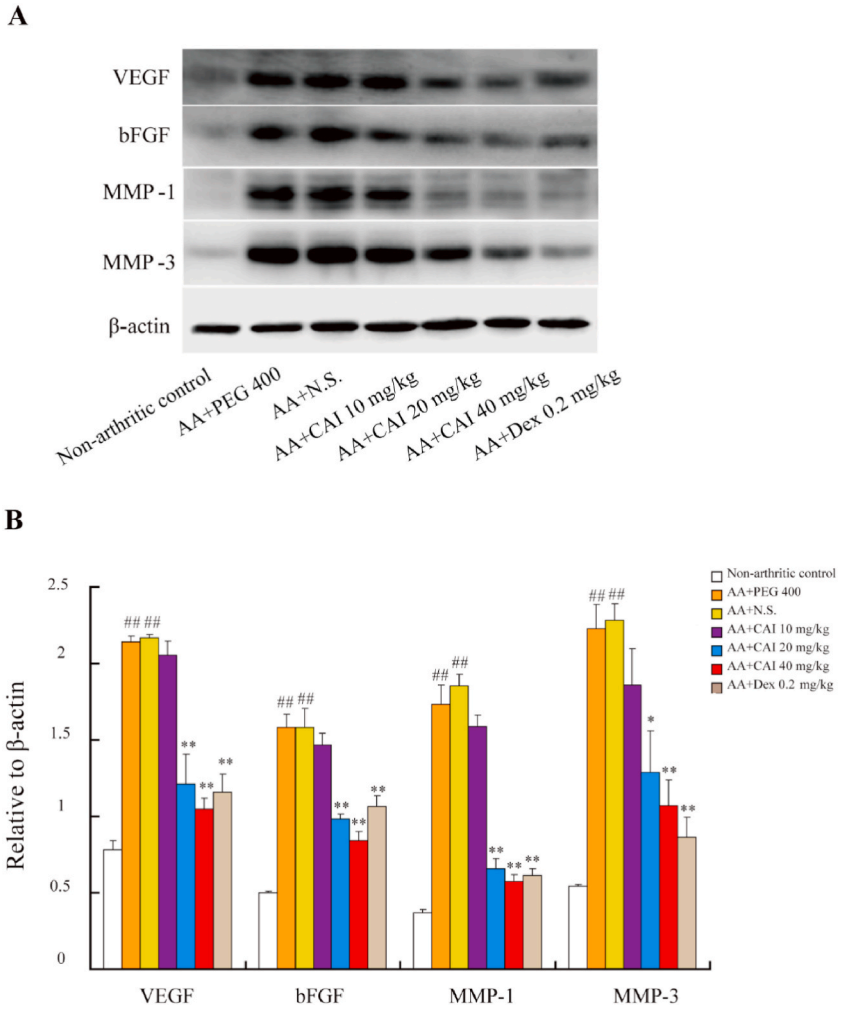

Fig. 6. Effect of CAI on the production of VEGF, bFGF, MMP-1 and MMP-3 in AA rats.

3.5. Effects of CAI on MAPK signaling pathway in AA rats

MAPK family members, such as p38, JNK, and ERK, regulate the expression of inflammatory cytokines and play pivotal roles in RA pathogenesis. To obtain insight into whether the inhibitory effect of CAI on AA was related to the regulation of the MAPK signaling pathway, we measured the protein expression of p38, JNK1/2, ERK1/2, and phosphorylated p38, JNK1/2, and ERK1/2 using Western blot analysis. Phosphorylation of p38, JNK, and ERK is elevated in AA models. Total levels of p38, JNK, and ERK did not change after CAI or Dex treatment. Nevertheless, CAI (20 and 40 mg/kg) or Dex (0.2 mg/kg) treatment suppressed the phosphorylation of p38, JNK1/2, and ERK1/2 compared to that in the control group (Fig. 5A and B). These results suggested that the inhibitory effects of CAI on AA in rats were associated with the MAPK pathway.

3.6. Effects of CAI on the levels of VEGF, bFGF, MMP-1, and MMP-3 in AA rats

In response to infectious factors and other environmental factors presented inside and outside of RA, angiogenic factors, such as VEGF and bFGF, act on the pathogenesis of synovial angiogenesis. In addition to VEGF and bFGF, MMPs, particularly MMP-1 and MMP-3, are also found at high levels in RA synovial tissues, which are thought to lead to the destruction of cartilage and other correlative components. Thus, we determined the levels of VEGF, bFGF, MMP-1, and MMP-3 in the synovial tissue of AA rats using

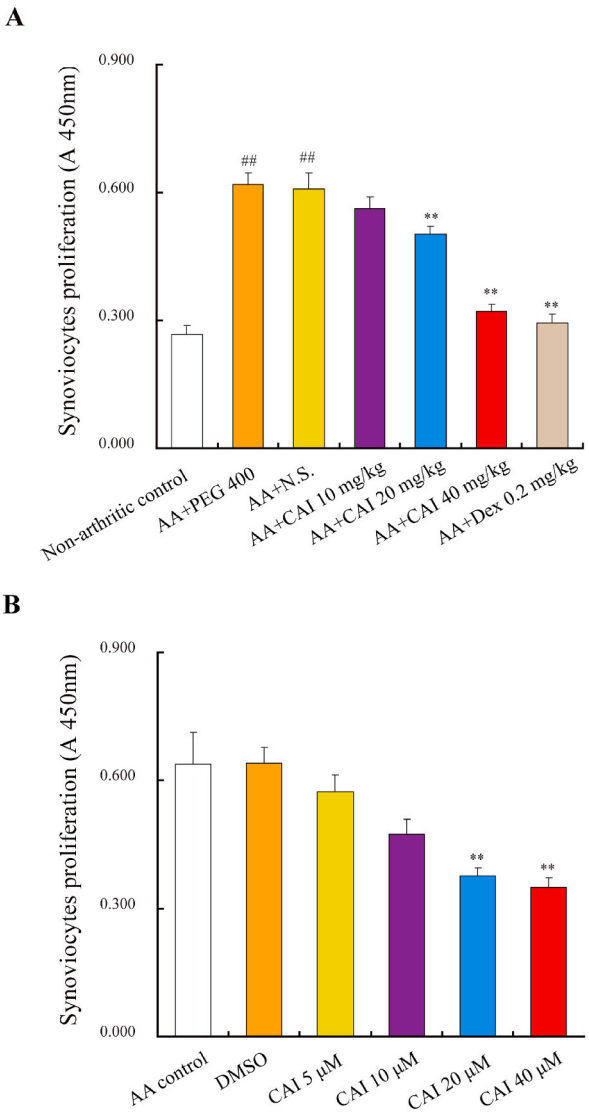

Fig. 7. Effect of CAI on FLS proliferation A. FLS isolated from indicated CAI treatment AA rats were incubated for 24 h. B. FLS isolated from AA rats were incubated for 24 h, and then indicated concentrations of CAI were treated with for 48 h. FLS proliferation was determined by the CCK-8 assay as described in Materials and Methods. n = 3, Mean ± SD. $^{\#\#}P < 0.01$ *vs.* non-arthritic control group, $^{**}P < 0.01$ *vs.* vehicle-treated AA group.

Western blot analysis. The results suggested that the production of VEGF, bFGF, MMP-1, and MMP-3 increased in AA rats, whereas the production in AA rats treated with CAI (20, 40 mg/kg) or Dex (0.2 mg/kg) decreased than that in the vehicle PEG 400- and N.S.-treated AA rats (Fig. 6A and B). These results were consistent with the findings of the histopathological assessment and new blood vessel examination, which confirmed the inhibitory effect of CAI on bone erosion and angiogenesis in the AA model.

Synovial tissues from the indicated groups of rats were homogenized from the joints on day 26 in ice-cold lysis buffer, and pellets were prepared for Western blot analysis of expression changes. (A) Western blot analysis of VEGF, bFGF, MMP-1, and MMP-3 in AA rats treated with different CAI concentrations (original image seeing in supplementary Fig 6A). B: Bar graphs show quantitative evaluation of VEGF, bFGF, MMP-1, and MMP-3 bands by densitometry in triplicate independent experiments. $^{\#\#}P < 0.01$ *vs.* non-arthritic control group; $^{*}P < 0.05$, $^{**}P < 0.01$ *vs.* vehicle-treated AA group.

3.7. Effects of CAI on FLS proliferation in vivo and in vitro

Abnormal proliferation of FLS is frequently observed in RA, and it plays an important role in the production of inflammatory mediators, such as proinflammatory cytokines and MMPs. FLS can be activated by a series of cytokines, and the proliferated FLS, in turn, aggravate synovial inflammation, subsequently contributing to the perpetuation of cartilage and bone destruction during RA development. To investigate the effect of CAI on the proliferation of FLS *in vivo*, FLS were isolated from AA rats under different treatment conditions, and their proliferation was measured using the CCK-8 assay. The results showed that while FLS proliferation occurred in AA rats, it was significantly impeded by CAI (20 and 40 mg/kg) or Dex (0.2 mg/kg) treatment compared to that observed with the PEG 400 or N.S. treatment (Fig. 7A). Then, we explored the function of CAI on FLS proliferation of AA *in vitro*. Isolated FLS from AA rats were treated with CAI at various final concentrations of 5, 10, 20, and 40 μM for 48 h in three independent experiments. CCK-8 assay revealed that CAI (20 and 40 μM) inhibited the proliferation of FLS in a concentration-dependent manner compared with DMSO control (Fig. 7B). Finally, we demonstrated that CAI inhibited FLS proliferation both *in vivo* and *in vitro*, which may be a critical stage at which joint protection was mediated.

4. Discussion

Human RA is a multiple systemic inflammatory disease that affects 0.5–1% of the population globally. RA primarily influences the lining of the synovial tissues and is characterized mainly by synovitis and pannus formation, resulting in structural damage to joints [14]. But for a long time, conventional treatments for RA demonstrated unsatisfactory side effects. Hence, the development of agents with good effects and minor side effects were required [15,16]. CAI is a chemical compound that has been studied for a long term and has been widely applied to treat cancer in combination with other anticancer drugs in varieties of preclinical reports and clinical trials [17–21]. Recently, a series of preclinical experiments demonstrated the anti-inflammatory and immunomodulatory properties of CAI [10,11,22,23]. In this study, we assessed the therapeutic effects in an AA model, the most universally studied animal model of arthritis, reproducing human RA clinical and pathological manifestations [24]. Our results showed weight protection by CAI at the early stages of arthritis, in contrast to the positive control, Dex. Up to day 26, the group treated with CAI showed a return of body weight to basal levels. In addition, Dex showed no weight recovery. A previous study demonstrated the protective effects of CAI against inflammatory syndromes and joint pathological changes in rats with AA [25]. Based on the aforementioned results, our study further showed that CAI exhibited a significant inhibitory effect on pannus formation in AA. This finding implies its potentially protective effect on joint erosion.

During the pathological progression of RA, angiogenesis, characterized by the generation of new capillaries providing a blood supply to the pannus found at the interface with the cartilage and bone, plays a pivotal role in causing synovial hyperplasia and progressive bone destruction [26,27]. Thus, the identification of agents that inhibit angiogenesis may represent a potential approach for the treatment of RA. There is strong evidence that angiogenesis inhibitors offer effective protection against synovial inflammation and bone destruction in mice with antigen-induced arthritis (AIA) [28]. In this study, CAI showed significant pharmacological efficacy in ameliorating pathological changes and decreasing the number of new blood vessels. Immunohistochemical staining for CD31, a surface marker of blood vessels, was performed to confirm that CAI suppressed angiogenesis in AA rats.

The MAPK pathway, which involves three individual subfamilies, p38, JNK, and ERK, controls a series of reactions to harmful external pathogens. In RA, MAPK proteins are expressed in macrophages and synoviocytes and regulate the production and action of cytokines and MMPs as well as the behavior of FLS. MAPK helps in the CXCL16-mediated recruitment to rheumatoid arthritis synovial tissue and murine lymph nodes [29]. MAPK signaling is essential in the initial stages of osteoclastogenesis [30,31]. A large number of MAPK inhibitors have been developed as new drugs for rheumatoid arthritis over recent years [32]. In the current study, we observed that CAI regulated the MAPK signaling pathway by inhibiting the phosphorylation of p38, JNK, and ERK, which may explain the systemic protective effects of CAI in AA rats.

Growth factors, such as VEGF and bFGF, are excessively expressed in the synovium of RA and are the key regulators of angiogenesis. They are involved in the proliferation and migration of vascular endothelial cells, vascular tube formation, and prevention of endothelial cell apoptosis [33]. VEGF is a multifunctional factor that is a potent mediator of vascular permeability and enhances angiogenesis and pannus formation. Another significant pro-angiogenic factor, bFGF, is a potent mitogen and chemoattractant for endothelial cells and fibroblasts [34,35]. In this study, we demonstrated that the production of VEGF and bFGF in AA rats treated with CAI was lower than that in the synovial tissue lysates from vehicle-treated AA rats. Thus, we concluded that CAI prevents the destruction of the joints of AA rats partly due to the blocking of angiogenesis by suppressing the generation of angiogenic factors VEGF and bFGF.

MMPs are a family of zinc-containing, calcium-dependent proteinases that maintain a balance with MMPs inhibitors in the synovial fluid of normal joints [36]. However, MMPs, especially MMP-1 and MMP-3, are overexpressed by FLS in RA tissues. MMP-1 and MMP-3 can break down and digest the joint basement membrane and ECM components, which are closely associated with joint destruction and subsequent severe deformity [37]. MMP-1, also known as fibroblast type or interstitial collagenase, can cleave native type I, II, and III collagen. MMP-3, also known as stromelysin-1, is a broader substrate of ECM components in joints. Notably, MMP-1 can be expressed by both synovial fibroblasts and chondrocytes, whereas MMP-3 is barely expressed by synovial fibroblasts from rheumatoid joints. In RA, MMP-1 and MMP-3 production is regulated by growth factors and cytokines via the modulation of their gene expression. Therefore, more researchers consider them to be predominant proteinases that contribute to synovial hyperplasticity and cartilage damage, thus causing pannus formation [35,38]. Our results revealed that CAI suppressed MMP-1 and MMP-3 expression in the lysed synovial tissue of AA rats. This result is consistent with that of our histopathological examination, which showed that CAI protected against synovial hyperplasia and cartilage loss in AA rats.

Moreover, notably, there is an activated phenotypic change in FLS within the RA synovium, which displays hyperplastic, aggressive, and invasive behaviors and involves the formation of pannus [39]. In this study, we examined the proliferation of CAI-treated FLS under conditions involving AA *in vivo* and untreated FLS following CAI treatment *in vitro* and found that cell proliferation was impeded. These results indicate that CAI might slow the progression of bone destruction, depending on its anti-proliferative effect on FLS.

In this study, we explored the therapeutic effects and mechanisms of joint destruction of AA rats. Previous reports have demonstrated the remarkable protective effect of CAI on AA arthritis. Here, we further demonstrated that abnormal joint phenotypes, including angiogenesis, hyperplasia, and cartilage erosion were also inhibited by CAI via suppression of the activation of the MAPK signaling pathway, impeding the production of VEGF, bFGF, MMP-1, and MMP-3 from synoviocyte populations and controlling of FLS proliferation. In conclusion, our research shows that CAI is a potent agent for treating AA by alleviating pannus formation and cartilage erosion, which implies that CAI might be a potential candidate drug for treating patients with RA.

Author contribution statement

Lei Zhu: Conceived and designed the experiments; Wrote the paper; Contributed reagents, materials, analysis tools or data.
Caiying Ye: Conceived and designed the experiments.
Yongting Zhou: Performed the experiments; Contributed reagents, materials, analysis tools or data; Wrote the paper.
Xiyue Yang: Performed the experiments; Contributed reagents, materials, analysis tools or data.
Jingwen Liu, Mei Yang: Performed the experiments.

Data availability statement

Data included in article/supp. material/referenced in article.

Additional information

No additional information is available for this paper.

Ethics statement

All animal experiments were approved by the Institutional Animal Care and Use Committee of Chinese Academy of Medical Science (ACUC-A02-2021-027).

Funding statement

This study was supported by the Chinese National Key Technology R&D Program, Ministry of Science and Technology (2017YFC0907601, 2017YFC0907604 , 2019YFC08040603) , Chinese Academy of Medical Sciences (CAMS) Innovation Fund for Medical Sciences (CIFMS) (2021-I2M-1–005), the Non-profit Central Research Institute Fund of Chinese Academy of Medical Sciences (2019PT330004)

Availability of data and materials

The datasets used and/or analyzed in this study are available from the corresponding author on reasonable request.

Declaration of competing interest

The authors declare that they have no known competing financial interests or personal relationships that could have appeared to influence the work reported in this paper.

Acknowledgements

Not applicable.

Appendix A. Supplementary data

Supplementary data to this article can be found online at https://doi.org/10.1016/j.heliyon.2023.e20105.

References

[1] M.P. van der Linden, K.le Cessie S. Raza, et al., Long-term impact of delay in assessment of patients with early arthritis, Arthritis Rheum. 62 (2010) 3537–3546.
[2] N.Takayanagi H. Komatsu, Mechanisms of joint destruction in rheumatoid arthritis - immune cell-fibroblast-bone interactions, Nat. Rev. Rheumatol. 18 (2022) 415–429.
[3] H. Takayanagi, Osteoimmunology: shared mechanisms and crosstalk between the immune and bone systems, Nat. Rev. Immunol. 7 (2007) 292–304.
[4] Q. Huang, Y. Ma, A. Adebayo, et al., Increased macrophage activation mediated through toll-like receptors in rheumatoid arthritis, Arthritis Rheum. 56 (2007) 2192–2201.
[5] H. Liu, Y. Zhu, Y. Gao, et al., NR1D1 modulates synovial inflammation and bone destruction in rheumatoid arthritis, Cell Death Dis. 11 (2020) 129–146.
[6] F. Mizoguchi, K. Slowikowski, K. Wei, et al., Functionally distinct disease-associated fibroblast subsets in rheumatoid arthritis, Nat. Commun. 9 (2018) 789–799.
[7] F. Sabeh, D. Fox, S.J. Weiss, Membrane-type I matrix metalloproteinase-dependent regulation of rheumatoid arthritis synoviocyte function, J. Immunol. 184 (2010) 6396–6406.
[8] M.F. Bustamante, R. Garcia-Carbonell, K.D. Whisenant, et al., Fibroblast-like synoviocyte metabolism in the pathogenesis of rheumatoid arthritis, Arthritis Res. Ther. 19 (2017) 110–121.
[9] M.I. Koenders, W.B. van den Berg, Novel therapeutic targets in rheumatoid arthritis, Trends Pharmacol. Sci. 36 (2015) 189–195.
[10] L. Zhu, J. Li, L. Guo, et al., Activation of NALP1 inflammasomes in rats with adjuvant arthritis; a novel therapeutic target of carboxyamidotriazole in a model of rheumatoid arthritis, Br. J. Pharmacol. 172 (2015) 3446–3459.
[11] S. Lu, M. Duan, Z. Guo, et al., Carboxyamidotriazole exerts anti-inflammatory activity in lipopolysaccharide-induced RAW264.7 macrophages by inhibiting NF-κB and MAPKs pathways, Exp. Ther. Med. 20 (2020) 1455–1466.
[12] Q. Gao, J. Shan, L. Di, et al., Therapeutic effects of daphnetin on adjuvant-induced arthritic rats, J. Ethnopharmacol. 120 (2008) 259–263.
[13] L. Zhu, W. Wei, Y.Q. Zheng, et al., Effects and mechanisms of total glucosides of paeony on joint damage in rat collagen-induced arthritis, Inflamm. Res. 54 (2005) 211–220.
[14] G. Nygaard, G.S. Firestein, Restoring synovial homeostasis in rheumatoid arthritis by targeting fibroblast-like synoviocytes, Nat. Rev. Rheumatol. 16 (2020) 316–333.
[15] A.J. Silman, J.E. Pearson, Epidemiology and genetics of rheumatoid arthritis, Arthritis Res. 4 (Suppl 3) (2002) S265–S272.
[16] Q. Guo, Y. Wang, D. Xu, et al., Rheumatoid arthritis: pathological mechanisms and modern pharmacologic therapies, Bone Res 6 (2018) 15–28.
[17] W.J. Wasilenko, A.J. Palad, K.D. Somers, et al., Effects of the calcium influx inhibitor carboxyamido-triazole on the proliferation and invasiveness of human prostate tumor cell lines, Int. J. Cancer 68 (1996) 259–264.
[18] T.W. Moody, J. Chiles, E. Moody, et al., CAI inhibits the growth of small cell lung cancer cells, Lung Cancer 39 (2003) 279–288.
[19] M.M. Hussain, H. Kotz, L. Minasian, et al., Phase II trial of carboxyamidotriazole in patients with relapsed epithelial ovarian cancer, J. Clin. Oncol. : Official Journal of the American Society of Clinical Oncology 21 (2003) 4356–4363.
[20] J.P. Dutcher, L. Leon, J. Manola, et al., Phase II study of carboxyamidotriazole in patients with advanced renal cell carcinoma refractory to immunotherapy: E4896, an Eastern Cooperative Oncology Group Study, Cancer 104 (2005) 2392–2399.
[21] T. Mikkelsen, R. Lush, S.A. Grossman, et al., Phase II clinical and pharmacologic study of radiation therapy and carboxyamido-triazole (CAI) in adults with newly diagnosed glioblastoma multiforme, Invest. N. Drugs 25 (2007) 259–263.
[22] X. Du, W. Chen, Y. Wang, et al., Therapeutic efficacy of carboxyamidotriazole on 2,4,6-trinitrobenzene sulfonic acid-induced colitis model is associated with the inhibition of NLRP3 inflammasome and NF-kappaB activation, Int. Immunopharm. 45 (2017) 16–25.
[23] R. Ju, D. Wu, L. Guo, et al., Inhibition of pro-inflammatory cytokines in tumour associated macrophages is a potential anti-cancer mechanism of carboxyamidotriazole, Eur. J. Cancer 48 (2012) 1085–1095. Oxford, England : 1990.
[24] K. Kannan, R.A. Ortmann, D. Kimpel, Animal models of rheumatoid arthritis and their relevance to human disease, Pathophysiology 12 (2005) 167–181.
[25] L. Zhu, J. Li, L. Guo, et al., Therapeutic effect of carboxyamidotriazole on adjuvant arthritis in rats, Zhongguo Yi Xue Ke Xue Yuan Xue Bao 38 (2016) 49–54.
[26] Y. Wang, H. Wu, R. Deng, Angiogenesis as a potential treatment strategy for rheumatoid arthritis, Eur. J. Pharmacol. 910 (2021) 174500–174514.
[27] H.A. Elshabrawy, Z. Chen, M.V. Volin, et al., The pathogenic role of angiogenesis in rheumatoid arthritis, Angiogenesis 18 (2015) 433–448.
[28] Q. Chen, K. Fan, X. Chen, et al., Ezrin regulates synovial angiogenesis in rheumatoid arthritis through YAP and Akt signalling, J. Cell Mol. Med. 25 (2021) 9378–9389.
[29] J.H. Ruth, C.S. Haas, C.C. Park, et al., CXCL16-mediated cell recruitment to rheumatoid arthritis synovial tissue and murine lymph nodes is dependent upon the MAPK pathway, Arthritis Rheum. 54 (2006) 765–778.
[30] T. Miyazaki, H. Katagiri, Y. Kanegae, et al., Reciprocal role of ERK and NF-kappaB pathways in survival and activation of osteoclasts, J. Cell Biol. 148 (2000) 333–342.
[31] M. Matsumoto, T. Sudo, T. Saito, et al., Involvement of p38 mitogen-activated protein kinase signaling pathway in osteoclastogenesis mediated by receptor activator of NF-kappa B ligand (RANKL), J. Biol. Chem. 275 (2000) 31155–31161.
[32] S. Liu, H. Ma, H. Zhang, et al., Recent advances on signaling pathways and their inhibitors in rheumatoid arthritis, Clin. Immunol. 230 (2021), 108793.
[33] A. Marrelli, P. Cipriani, V. Liakouli, et al., Angiogenesis in rheumatoid arthritis: a disease specific process or a common response to chronic inflammation? Autoimmun. Rev. 10 (2011) 595–598.
[34] P.A. Klimiuk, S. Sierakowski, R. Latosiewicz, et al., Soluble adhesion molecules (ICAM-1, VCAM-1, and E-selectin) and vascular endothelial growth factor (VEGF) in patients with distinct variants of rheumatoid synovitis, Ann. Rheum. Dis. 61 (2002) 804–809.
[35] S. Fromm, C.C. Cunningham, M.R. Dunne, et al., Enhanced angiogenic function in response to fibroblasts from psoriatic arthritis synovium compared to rheumatoid arthritis, Arthritis Res. Ther. 21 (2019) 297–307.
[36] G. Murphy, V. Knäuper, S. Atkinson, et al., Matrix metalloproteinases in arthritic disease, Arthritis Res. 4 (Suppl 3) (2002) S39–S49.
[37] T.C.A. Tolboom, E. Pieterman, W.H. van der Laan, et al., Invasive properties of fibroblast-like synoviocytes: correlation with growth characteristics and expression of MMP-1, MMP-3, and MMP-10, Ann. Rheum. Dis. 61 (2002) 975–980.
[38] M.P. Vincenti, C.E. Brinckerhoff, Transcriptional regulation of collagenase (MMP-1, MMP-13) genes in arthritis: integration of complex signaling pathways for the recruitment of gene-specific transcription factors, Arthritis Res. 4 (2002) 157–164.
[39] E. Neumann, S. Lefèvre, B. Zimmermann, et al., Rheumatoid arthritis progression mediated by activated synovial fibroblasts, Trends Mol. Med. 16 (2010) 458–468.